

B. MIKUŁOWSKI\*, R. ZAPAŁA\*\*, J. GŁOWNIA\*\*, P. WILK\*

## STRUCTURE AND PROPERTIES OF THE CENTRIFUGALLY CAST HIGH-ALLOYED (25Cr35NiNbTi) STEEL AFTER LONG-TIME OPERATION IN STEAM REFORMING

## STRUKTURA I WŁASNOŚCI ODLEWANEGO ODŚRODKOWO WYSOKOSTOPOWEGO STALIWA (25Cr35NiNbTi) PO WIELOLETNIEJ EKSPLOATACJI W REFORMINGU PAROWYM

The paper presents the influence of performance conditions of high-alloyed nickel-chromium cast steel intended for use in steam reforming plants on the morphology and number of phases present in centrifugally cast tubes. Structure identification was done by the methods of light and scanning microscopy. It was found that the main components of the tested cast steel microstructures are carbides of, among others, chromium, iron, and niobium. The structure has also been reported to contain the sigma phase. Additionally, at three test temperatures (20, 820 and 945°C), the mechanical properties of the cast steel were determined after years of operation under industrial conditions. The tested material was characterised by low, compared with standard requirements, mechanical properties. A relationship between the content of phases (primary and secondary carbides), measured by the methods of quantitative metallography, and the yield strength of the tested material was determined. The yield strength determined at room temperature, and at 820°C and 945°C assumed higher values in samples characterised by a relatively large volume content of phases.

*Keywords:* steam reforming, alloyed cast steel, primary and secondary carbides, volume content of phases, mechanical properties

W pracy przedstawiono wpływ warunków eksploatacji wysokostopowego staliwa niklowo-chromowego przeznaczonego do pracy w instalacjach reformingu parowego na morfologię oraz ilość faz występujących w materiale rur odlewanych odśrodkowo. Do identyfikacji struktury wykorzystano metody mikroskopii świetlnej i skaningowej. Ponadto w trzech temperaturach badań (20, 820 i 945°C) określono własności mechaniczne staliwa po eksploatacji w warunkach przemysłowych. Wyznaczono związek pomiędzy ilością faz (węglików pierwotnych i wtórnych), określoną przy wykorzystaniu metody metalografii ilościowej, a umowną granicą plastyczności badanego materiału.

### 1. Introduction

The failure-free time of operation of an installation, i.e. the service life, depends on many factors, which may include, among others, temperature and time of operation, the type of atmosphere (oxidising and carburising), stress, the type of furnace design, the type of material and technology used in the manufacture of a given item. In reforming installations, the most susceptible to damages are tubes, in which the endothermic chemical reactions (e.g. the decomposition of natural gas to hydrogen and carbon monoxide) take place. Tubes operating in steam reforming plants are designed for up to 100,000 hours of operation, at a maximum temperature of 945°C and pressure inside the pipe not exceeding 4 MPa [1, 2].

These tubes are made of high carbon, austenitic, nickel-chromium cast steel. Nickel is added to provide a stable austenitic structure and resistance to carburisation, while chromium should provide an adequate high-temperature cor-

rosion resistance. Other alloying elements (among others Nb, Ti, Co, W, Zr) are introduced to the cast steel to harden the austenite, to produce secondary precipitates hardening the matrix, and to increase the size of austenite grains. The ultimate goal is to produce material with adequate creep resistance.

The highest degree of the solution hardening of austenite is achieved with additions of nitrogen and boron, forming interstitial solutions with the alloy matrix. Tungsten and molybdenum, as long as are not bound in carbides, are also effective in austenite hardening, but increase the tendency of this alloy to the formation of a brittle  $\sigma$  phase. The least effective in the solution hardening of austenite are elements such as carbon (too low content of carbon dissolves in austenite [3]) and manganese and nickel. The precipitation hardening of alloyed nickel-chromium cast steel is proportional to the carbon content in alloy, because this element determines the amount of carbides formed in the material (e.g. chromium carbides or  $(Fe,Mn)_3C$ ). The ultimate creep resistance of the

\* AGH UNIVERSITY OF SCIENCE AND TECHNOLOGY DEPARTMENT OF METALLIC MATERIALS AND NANOENGINEERING, FACULTY OF NON-FERROUS METALS, AL. A. MICKIEWICZA 30, 30-059 KRAKÓW, POLAND

\*\* AGH UNIVERSITY OF SCIENCE AND TECHNOLOGY DEPARTMENT OF CAST ALLOYS AND COMPOSITES ENGINEERING, FACULTY OF FOUNDRY ENGINEERING, REYMONTA ST. 23, 30-059 KRAKÓW, POLAND

cast steel depends not only on the transformation of primary chromium carbides, which takes place during alloy performance, but also on the morphology (structure, size, position) of the secondary, inter- and transcrystalline  $M_{23}C_6$  type carbides. The  $M_{23}C_6$  type carbides precipitate on the austenite grain boundaries, resulting in hardening of the material. Yet, this effect is not permanent, and due to the dissolution and coagulation of carbides during aging, a continuous network of these compounds is formed at the matrix grain boundaries. This results in the formation of cracks and micropores at the carbide/alloy matrix phase boundary.

To increase the amount of the forming carbides, elements with high affinity to carbon (e.g. Nb, Ti) are introduced to the cast steel. Niobium and titanium form MC type carbides and increase the content of eutectic (carbide - austenite) at the austenite grain boundaries, increasing, in turn, the creep resistance as compared to nickel-chromium alloyed cast steel of unmodified chemical composition. It is worth noting that during long-term use of tubes, these carbides can offer much better stability than the secondary  $M_{23}C_6$  carbides, which lets them keep unchanged both size and position.

The improved creep resistance of cast steel due to the precipitation and solution hardening allows using tubes with smaller wall thicknesses. The reduced wall thickness helps to increase the durability of the tubing (lower temperature on the outer tube surface and reduced stress in the walls), improves process efficiency (increased yield of catalyst operating inside the tube), and reduces the amount of alloy necessary for the tube manufacture.

## 2. Test materials and methods

Samples used in this study were taken from the centrifugally cast tubes made of the heat-resistant 25Cr35NiNbTi steel (according to DIN EN 10027). The chemical composition of the tested cast steel is shown in Table 1. From the wall of the tube operating previously in a steam reforming unit, specimens were cut out for structure examinations and testing of mechanical properties. The designation of specimens, the operating conditions and tube sections where samples were taken are compared in Table 2.

TABLE 1  
Chemical composition of the examined cast steel according to DIN EN 10027

Grade	Chemical composition, wt%							
	C	Mn	Cr	Ni	Mo	Nb	Fe	Other elements
25Cr35NiNbTi	0.6	1.25	25	35	<0.25	0.8	rest	Ti, W, V < 0.02

Metallographic studies were carried out on specimens mechanically cut out with a high-precision Disotom-6 cutter made by Struers. Specimen surfaces perpendicular to the tube axis were etched with aqua regia containing 20 ml  $HNO_3$  and 60 ml  $HCl$ . For the initial identification of carbides, the  $Mi10Fe$  reagent (containing according to PN-61/H-04503 – 10g of potassium ferrocyanide, 10 g of potassium hydroxide, 100 ml of distilled water) was used. Structure in all the

examined pipe sections was observed under an AXIO Observer.Z1m light microscope made by Zeiss.

TABLE 2  
The designation of specimens and operating conditions of the tube sections where specimens were cut out

Designation of specimens	Tube sections where specimens were cut out	Operating parameters	
		Time [years/hours]	Approximate temperature [ $^{\circ}C$ ]
R1	lower part	5/42,500	1050 $^{\circ}C$
R2	middle part	5/42,500	800 $^{\circ}C$
R3	middle part	10/85,000	800 $^{\circ}C$

Additionally, the chemical composition of phases present in the cast steel structure after operation was analysed and carbide types were identified. The analysis was performed on a STEREOSCAN 420 scanning electron microscope with EDS attachment. In the studies, a 25 kV accelerating voltage and sample current of 350 pA were applied. Specimens for the scanning electron microscopy were prepared in the same way as for the observations under an light microscope, but polished sections were etched with aqua regia only.

The amount of carbide phases (primary and secondary) was measured by the method of symmetrically spaced points (the mesh method). The evaluation was performed on a mesh with 972 nodes. The number of mesh impositions was determined from equation (1).

$$k = \frac{u_{\alpha}^2(1 - V_v)}{\gamma^2 \cdot z \cdot V_v}, \quad (1)$$

where:

$V_v$  – the relative phase/constituent volume,

$z$  – the number of mesh points,

$\gamma$  – the relative error of analysis,

$u_{\alpha}$  – the value read out from the normal distribution table.

The relative error of analysis  $\gamma = 0.1$  was adopted with the  $1-\alpha = 0.9$  ( $\alpha = 0.1$ ) probability that it shall not exceed the preset value.

From the bottom (most heavy thermal load) and middle part of the tube, some segments were taken from which specimens for the mechanical tests were cut out parallel to the tube axis. The specimens were cut out from the tube wall centre. For mechanical tests, specimens of dimensions calculated from the results obtained in previous studies were used [4, 7, 8]. Testing of mechanical properties was performed at three temperatures, i.e. 20, 820 and 945 $^{\circ}C$ . The selection of test temperature was based on the cast steel operating conditions. Tensile tests were performed on an ST-SM Instron universal testing machine with an electronic measuring unit. The machine adapted to high temperature tests was equipped with a special Instron heating furnace of  $\pm 2^{\circ}C$  stability. The tensile tests were run at a speed of  $= 7 \cdot 10^{-4} s^{-1}$ . Using the results obtained, the  $\sigma = f(\epsilon)$  curves were plotted and were next used in calculations of the yield strength (YS) and tensile strength (TS). Unit elongation (EL) was also calculated.

Table 3 shows minimum mechanical properties as required for the tested cast steel by DIN EN 10027.

TABLE 3  
Nominal mechanical properties of the 25Cr35NiNbTi cast steel [5, 6]

Material	Minimum mechanical properties		
	YS [MPa]	TS [MPa]	EL [%]
25Cr35NiNbTi	230	470	8

### 3. Test results

High functional properties, creep resistance at high temperatures – in particular, of the 25Cr35NiNbTi steel in as-cast state are associated with the dendritic structure produced in tubes during casting. Figure 1 shows the structure of a sample taken from the test tube. The subsurface zone of fine grains (frozen crystals) has suffered degradation as a result of the impact of the work environment. It is interesting to note that the subsurface zone, which has suffered degradation, is wider (by about  $150\div 200\mu\text{m}$ ) in sample exposed to the effect of high temperature. The outer zone operating directly in the atmosphere of gas burners may undergo either decarburisation or carburisation, depending on conditions under which the production process is run. If the width of the decarburised or carburised layer does not exceed a few percent of the tube cross-section, it has no major effect on the casting properties [7, 8].

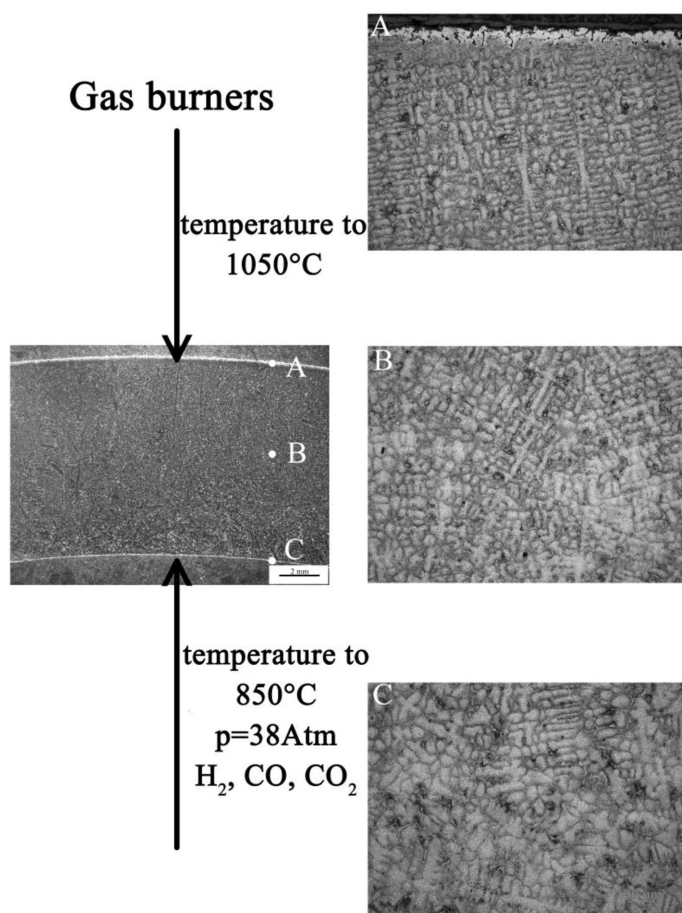


Fig. 1. Structures of tubes centrifugally cast from the 25Cr35NiNbTi steel after operation, aqua regia reagent

The zone of frozen crystals passes into a zone of columnar grains (Fig. 1A), whose orientation is due to the effect of centrifugal force during casting of tubes. In the inside part of the tube wall cross-section, the grains are equiaxed. Based on the conducted structural studies, it was found that despite the long operating time of the cast steel, the dendritic structure was not fully removed.

The main parameter contributing to the occurrence of adverse phase transformations, promoting changes in the tube structure, was high temperature operating in the bottom part of tube (sample designated as R1 – Table 2). The heat-induced changes in the tube structure resulted in carbides coagulation in the interdendritic spaces and in the appearance of secondary carbide precipitates in the austenite grains (Figs. 2 and 3).

In materials operating at  $800^\circ\text{C}$  for 42,500 and 85,000 hours, the precipitates appeared in the interdendritic spaces (carbide eutectic) and inside the dendrites on the whole tube wall cross-section (Fig. 2). Moreover, in some areas of the examined samples, fine-dispersed, irregular precipitates of the sigma phase in an austenitic matrix were observed.

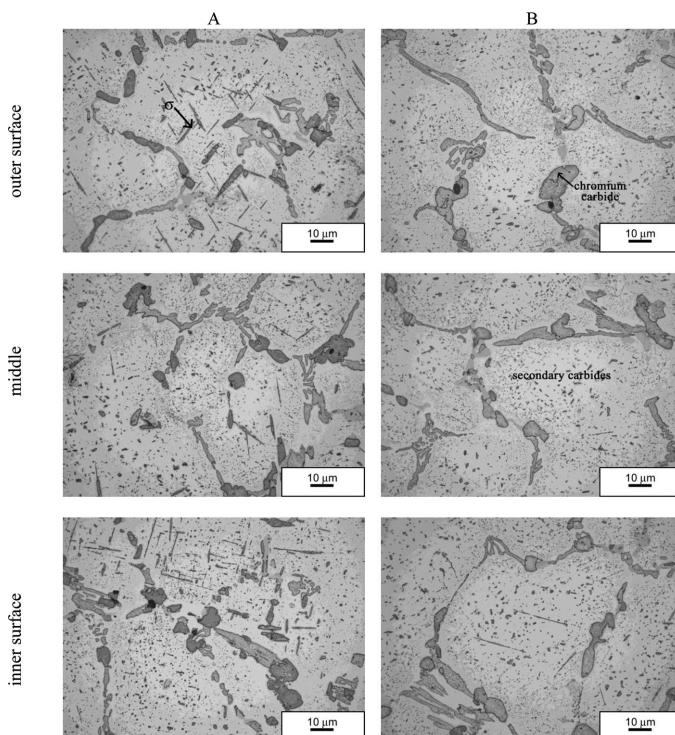


Fig. 2. Microstructure of tubes centrifugally cast from the 25Cr35NiNbTi steel after operation at temperatures of up to  $800^\circ\text{C}$  for 42,500 hours (A) and 85,000 hours (B), the Mi10Fe reagent, 1000x

Increasing the tube operating temperature changes the morphology of precipitates that are inside the dendrites (absence of lamellar precipitates) and results in partial coagulation of precipitates located in the interdendritic spaces (Fig. 3). It is worth noting that in all the examined samples, in the interdendritic spaces, due to the coagulation of carbides and high operating temperature of tubes, the appearance of micropores was observed (Figs. 2 and 3).

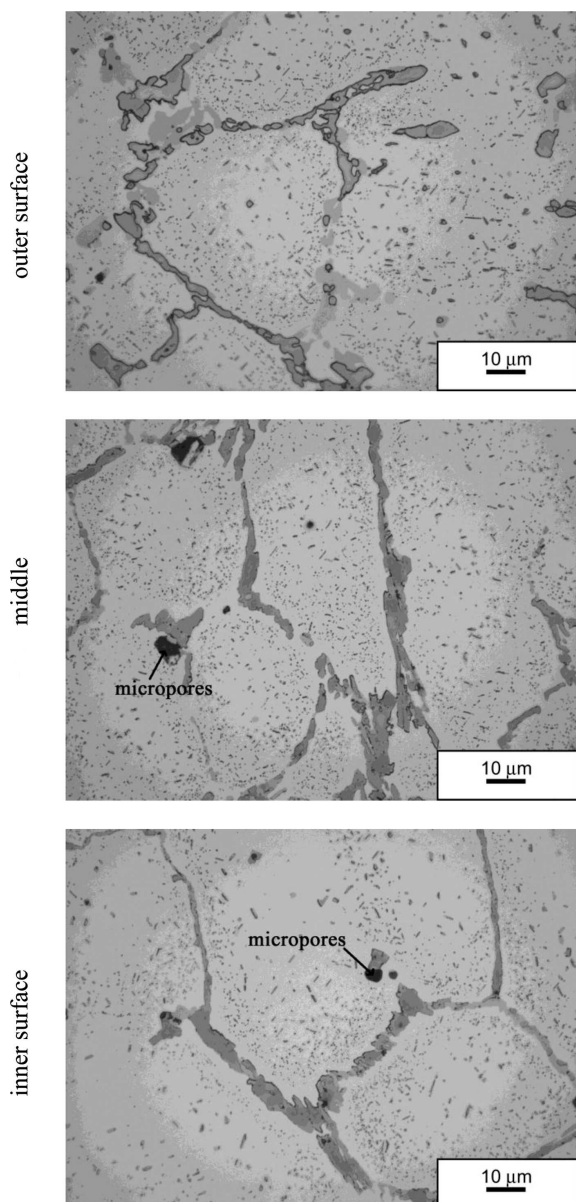


Fig. 3. Microstructure of tubes centrifugally cast from the 25Cr35NiNbTi steel after operation at temperatures of up to 1050°C for 42,500 hours, the Mi10Fe reagent, 1000x

In accordance with the images obtained during sample examination by scanning electron microscopy, in the interdendritic spaces, the occurrence of the phases of two types was detected. Light-colour precipitates were enriched with Nb and Si, while, compared to alloy matrix, dark colour precipitates were characterised by increased chromium content. Based on literature data it can be concluded that the chromium-containing phase is composed of chromium carbides of the  $M_{23}C_6$  type [9], while the niobium- and silicon-containing phase is the G phase, arising as a result of the  $NbC \rightarrow G$  phase ( $Ni_{16}Nb_6Si_7$ ) transformation [10, 11].

The structural changes discussed above have contributed to the decrease of mechanical properties in tubes made from the 25Cr35NiNbTi cast steel at a temperature of 20°C.

Table 4 compares the values of YS and TS obtained in the tensile test and the calculated unit elongation EL, while Figures 5 to 7 show these parameters in graphical form.

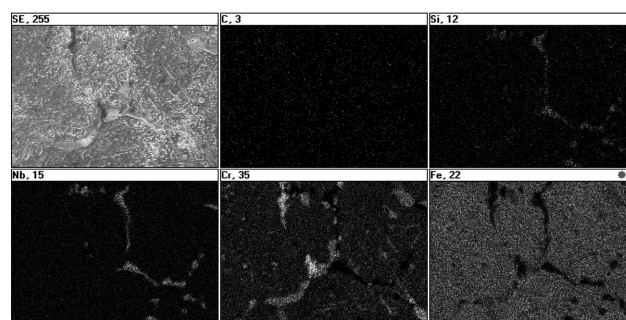
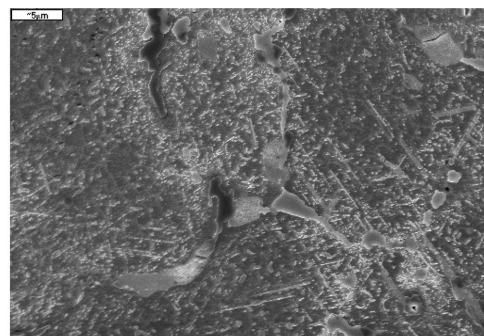


Fig. 4. Surface distribution of elements in microstructure of the 25Cr35NiNbTi cast steel after operation for 42,500 hours at temperatures of up to 800°C, the Mi10Fe reagent, SEM-EDS

TABLE 4

Tensile test results compared for a different test temperature

Sample designation	Test temperature [°C]	Mechanical properties		
		YS [MPa]	TS [MPa]	EL [%]
25Cr35NiNbTi	20	230	470	8
R1	20	376	430	3
	820	171	221	24
	945	97	120	29
R2	20	471	497	3
	820	202	250	16
	945	114	140	19
R3	20	432	441	2
	820	197	248	21
	945	113	134	27

Based on the analysis of the obtained results it has been concluded that the mechanical properties have decreased below the nominal values prescribed for the tested material. This is particularly evident in the case of plastic properties – the elongation at 20°C does not reach the nominal level required for this material. The reduced plastic properties of tubes resulted in the formation of micropores (poor compensation of internal stresses caused by temperature gradients that occur during the start-up and withdrawal of reformer, and also during its operation). Previous studies [7, 8] have shown that the safe time of the tube operation is when the decrease in YS and TS only slightly exceeds the nominal values, with EL never dropping below 50% of the nominal value prescribed for this type of material.

Based on the obtained results of mechanical testing, it was found that samples of the tested material taken from the bottom part of tubes operating at temperatures of up to 1050°C for 42,500 hours and at temperatures of up to 820°C for 42,500 hours and 85,000 hours, respectively, had different mechanical properties. The material operating at a lower temperature but for a longer time had better strength properties than the material operating at a higher temperature for a shorter period of time. The mechanical properties of materials operating at the same temperature but for different time periods also showed some differences. The material operating for 42,500 hours had better mechanical properties than the material operating for 85,000 hours.

The elongation of the material tested at room temperature was small and, depending on the sample, amounted to 2 or 3%. It increased with the increasing test temperature. At 820°C, the value of elongation was in the range of 16 to 24%, while at 945°C this range was from 19 to 29%. The lowest values of elongation at the temperatures of 820°C and 945°C had the samples operating for 42,500 hours (R2). This is probably associated with the occurrence in the tested material of small and irregular precipitates of the sigma phase [12, 13].

At the same time, the values of the tensile strength (TS) and yield strength (YS) were decreasing with the increasing test temperature (Table 4). At a temperature of 945°C, the yield strength reached 24 to 26% and the tensile strength 28÷30% of the value of these parameters at 20°C.

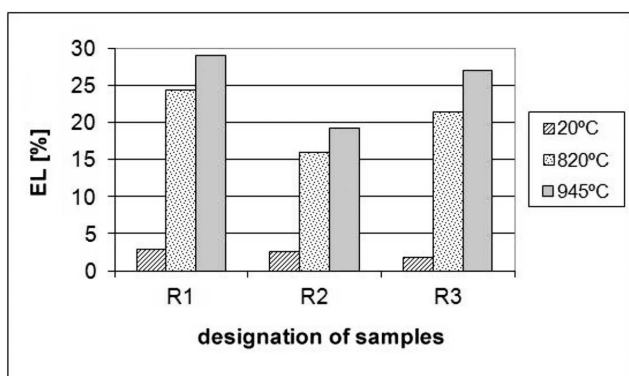


Fig. 5. Comparison of the values of elongation (EL) obtained for the 25Cr35NiNbTi cast steel after operation at different test temperatures

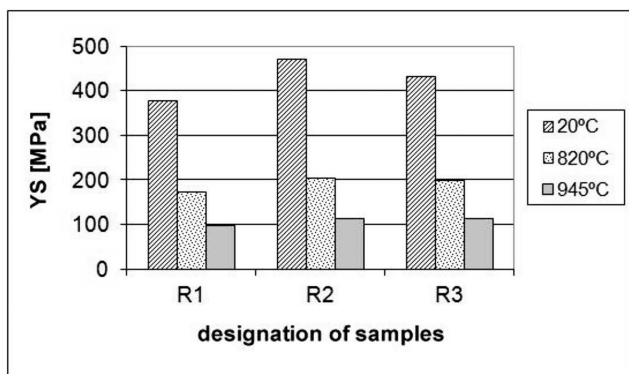


Fig. 6. Changes in the yield strength (YS) of the 25Cr35NiNbTi cast steel after operation at different test temperatures

This is confirmed by the data available in literature, according to which, up to 700°C, the elongation does not exceed 6%, and above this temperature it increases quite obviously; at the same time, both TS and YS reveal a mild decrease at temperatures of up to 820°C, to drop very violently when this level is exceeded [4, 14]. The changes result from the differences in the morphology of carbides present in the cast steel matrix.

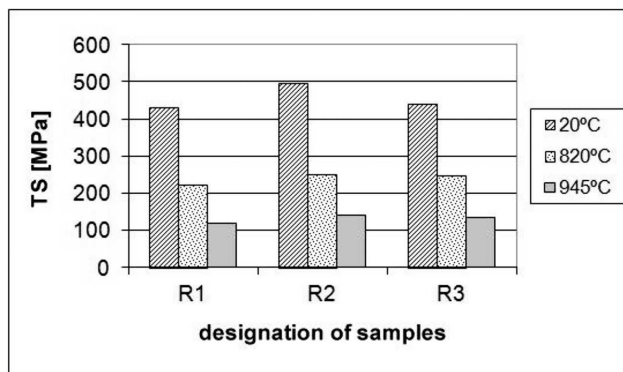


Fig. 7. Changes in the tensile strength (TS) of the 25Cr35NiNbTi cast steel after operation at different test temperatures

Table 5 compares the relative volume content of phases present in the alloy, and the obtained values of the yield strength. It was found that an increase in the relative volume of phases present in the cast steel contributed to an increase of the yield strength not only at room temperature but also at 820 and 945°C.

TABLE 5  
Volume content of phases in the middle of the sample and values of the yield strength

Sample designation	Relative volume content of phases [%]		Test temperature [°C]	YS [MPa]
	Primary precipitates	Secondary precipitates		
R1	7,27±0,314%	3,68±0,181	20	376
			820	171
			945	97
R2	8,36±0,336	4,38±0,198	20	471
			820	202
			945	114
R3	9,57±0,246	4,23±0,193	20	432
			820	197
			945	113

#### 4. Conclusions

Based on the studies of selected fragments of the reformer tubes centrifugally cast from the 25Cr35NiNbTi steel, the following conclusions were drawn:

1. The structure of the examined tubes is characterised by the occurrence of a large area of the coagulated carbides of chromium, iron and niobium present in the interdendritic

spaces, and secondary carbide precipitates inside the dendrites. In samples after operation at temperatures of up to 800°C, the structure additionally contains the sigma phase and micropores present in the interdendritic spaces.

2. Despite varying time and conditions of operation, the tested tubes have similar and very low, compared with the standard requirements, mechanical properties (YS, TS, EL).
3. In cast steel samples characterised by a relatively high volume content of phases, the yield strength at room temperature, and at 820 and 945°C assumes higher values than in the samples with a lower volume content of phases.

#### Acknowledgements

The research part of the study has been executed under a Statutory work no. 11.11.180.255.

#### REFERENCES

- [1] J.R. Rostrup-Nielsen, Catalytic steam reforming, Berlin – Heidelberg – New York – Tokyo 1984.
- [2] J. Łabanowski, An assessment of the destruction process of catalytic tubes in the operations of methane reformers, Gdańsk 2003.
- [3] J. Barcik, Alloys used for pyrolytic tubes, Katowice 1995.
- [4] G. Tęcza, J. Głownia, Archives of Foundry Engineering **4**, 209 (2008).
- [5] Werkstofftabellen Schmidt-Clemens GmbH+Co, Edelsthalwerk Kaisera 1993.
- [6] Heat-Resistant Alloys for Hydrocarbon Processing, Manoir Industries 1997.
- [7] B. Mikułowski, L. Błaż, M. Michno, B. Marczevska, A. Chromcewicz, Structural examinations of IN519 material used for catalytic tubes, Study made by IP-PiM AGH University of Science and Technology on request of GOZG Zabrze, (1990). Unpublished.
- [8] B. Mikułowski, Metallographic and mechanical studies of catalytic tubes at ambient temperature and the operating temperature (12ANC40 cast steel). Study made by ZA Chorzów on request of ZA Puławy, (1995). Unpublished.
- [9] S.H. Khodamorad, D. Haghshenas Fatmehsari, H. Rezaie, A. Sadeghipour, Engineering Failure Analysis **21**, 1 (2012).
- [10] T. Sourmail, Materials Science and Technology **17**, 1 (2001).
- [11] B. Piekarski, Materials Characterization **47**, 181 (2001).
- [12] G.D. Soares, L.H. de Almeida, T.L. da Silveira, I. Le May, Materials Characterization **29**, 387 (1992).
- [13] L.H. de Almeida, A.F. Ribeiro, I. Le May, Materials Characterization **49**, 219 (2003).
- [14] W. Steinkusch, Materials and Corrosion **49**, 69 (1998).